# Evaluation of Physicochemical Characteristics and Antimicrobial Activities of Copper Oxide Nanoparticles Formed by the Solution Combustion Method

A. Jegatha Christy
*Research Center of Physics, Jayaraj Annapackiam College for Women (Autonomous),*
Periyakulam, Theni district,India.
jegathachristy@gmail.com

Suresh Sagadevan
*Nanotechnology & Catalysis Research Centre,*
*Universiti Malaya,*
Kuala Lumpur, Malaysia
drsureshnano@gmail.com

Yasmin Abdul Wahab
*Nanotechnology & Catalysis Research Centre,*
*Universiti Malaya,*
Kuala Lumpur, Malaysia
yasminaw@um.edu.my

L. C. Nehru
*Department of Medical Physics, Bharathidasan University*,
Trichy, Tamilnadu, India.
lcnehru@bdu.ac.in

Hanim Hussin
*Faculty of Electrical Engineering,*
*Universiti Teknologi MARA,*
Shah Alam, Malaysia.
hanimh@uitm.edu.my

Nurul Ezaila Alias
*School of Electrical Engineering,*
*Universiti Teknologi Malaysia,*
Johor Bahru, Malaysia.
ezaila@fke.utm.my

Rozana Aina Maulat Osman
*Faculty of Electronic Engineering Technology,*
*Universiti Malaysia Perlis,*
Arau, Perlis, Malaysia.
rozana@unimap.edu.my

2021 IEEE Regional Symposium on Micro and Nanoelectronics (RSM) | 978-1-6654-1232-2/21/$31.00 ©2021 IEEE | DOI: 10.1109/RSM52397.2021.9511585

***Abstract*—In this paper, copper oxide (CuO) nanoparticles (NPs) was prepared by solution combustion technique. We used copper nitrate as an oxidizer and malic acid as a fuel to make three different CuO NPs by using different fuel ratios: low (M1), stoichiometric (M2), and high (M3). The XRD patterns show that the CuO NPs have the monoclinic structure with an average grain size of 17, 20, and 18 nm corresponding to M1, M2, and M3 respectively. The SEM images revealed that the CuO NPs prepared display bush as morphology consisting of a wheat-like structure for M1, rod-like structure for M2, and sheet-like structure for M3 sample. The FTIR spectrum shows that CuO NPs is successfully formed in all of the samples. A bandgap of around 3.26 eV can be seen in the UV-Vis spectrum. Also, the three samples are possessing antibacterial activity and are influenced by the crystalline size, shape, purity, and uniformity of the crystals. Among the three samples with a difference of morphology, the most influencing factor of antibacterial activity being the shape that of other larger-sized particles.**

**Keywords— CuO nanoparticles; Solution combustion method; Antimicrobial activity; Malic acid fuel.**

## I. INTRODUCTION

The nanotechnology principles and techniques help to create the next generation materials that are defect-free (unlike the existing ones) and can find applications in many different fields with many improvements to their fundamental properties [1-5]. Of various kinds of metal oxide NPs, the copper oxide (CuO) NPs because of the attractive physicochemical properties, are employed in catalysis, photoelectric diodes, Li-ion batteries, etc [6-10]. The sensory and antibacterial applications of this material are particularly attractive due to the good electrochemical activity and high specific surface area comparable to that of AgO; however, the AgO is relatively expensive and offers less oxidative stability (that of CuO) [11]. Also, the CuO NPs fall into the category of high ionic metal oxides and are particularly valuable as antimicrobial agents due to their preparation of extremely high surface areas and with unusual crystal morphologies [12]. Hence, for the preparation of CuO NPs, the commonly used methods include the sol-gel technique, combustion method, sonochemical method, electrochemical method, thermal decomposition, etc. and each method forms the NPs with different shapes, sizes, and morphology [13-14]. Such formed materials because of big differences in their properties exhibit a broad range of activities like antibacterial, photochemical, conductivity, magnetic behavior, etc.

Thus, the aim of this study is to investigate the activity of CuO NPs made by the same process but with different constituents, i.e., CuO NPs made by solution combustion were thoroughly investigated for structural, vibrational, and optical properties. The three different CuO NPs formed by changing the oxidizer to fuel ratio were investigated for their changes in crystallinity, morphology, and antibacterial activities.

978-1-6654-1232-2/21/$31.00 ©2021 IEEE

## II. EXPERIMENTAL PROCEDURE

### *A. Synthesis of CuO NPs*

The starting materials were taken from copper nitrate (Cu (NO3)2), malic acid (C4H6O5). For the synthesis, copper nitrate was first dissolved in deionized water, then malic acid fuel was added in stoichiometric quantities (M2). The solution was vigorously mixed until the homogeneous solution gets formed, and the solution remained at 250°C in the furnace. As the solution reaches the optimum temperature for combustion, it begins to burn, releasing a large amount of heat as fumes and vaporizing the whole solution. The combustion reaction took 15 minutes and resulted in the formation of fine black nanopowder. The same procedure was repeated by taking lower (M1) and higher amounts (M3) of malic acid fuel.

### *B. Antimicrobial study*

CuO NPs are tested for antimicrobial activity and were evaluated against gram-positive (B. cereus, and S. aureus), gram-negative bacteria (E. coli and K. pneumoniae), and fungi (P. chrysogenum). For the testing, four to five isolated colonies from each strain were first inoculated in 250 mL Erlenmeyer flasks containing 100 mL nutrient broth (for bacteria) and Saboraud Dextrose broth (fungi). Before inoculation, the strains were incubated at 37°C overnight on a rotary shaker (RS-24, REMI, India), and the turbidity of test cultures were set to the 0.5 McFarland norm. To obtain a standardized inoculum, a sterile and non-toxic swab was used to clean the suspension on the tube wall and streak it uniformly in three directions over the entire surface of Mueller Hinton Agar plates (MHA, HiMedia, India).

## III. RESULTS AND DISCUSSION

In this, we have generated three different CuO NPs formed by making use of copper nitrate (oxidizer) and malic acid (fuel) by making use of low (M1), stoichiometric (M2), and high (M3) ratios of oxidizer to the fuel. Figure 1 shows a comparison of XRD patterns of M1, M2, and M3 of CuO NPs, with sharp peak positions suggesting crystalline nature. From the XRD, the patterns are observed to the diffraction planes of (110), ($\bar{1}$11), (111), ($\bar{2}$02), (020), (202), ($\bar{1}$13), ($\bar{3}$11), (220), (311), and (004) respectively and is in accordance with the JCPDS no. 80-0076. Also, the observed diffraction peaks of CuO NPs for all the samples match well with the monoclinic structure. The Debye-Scherrer equation [15] was used to measure the average grain size of CuO NPs are 17 nm for M1, 20 nm for M2, and 18 nm for M3.

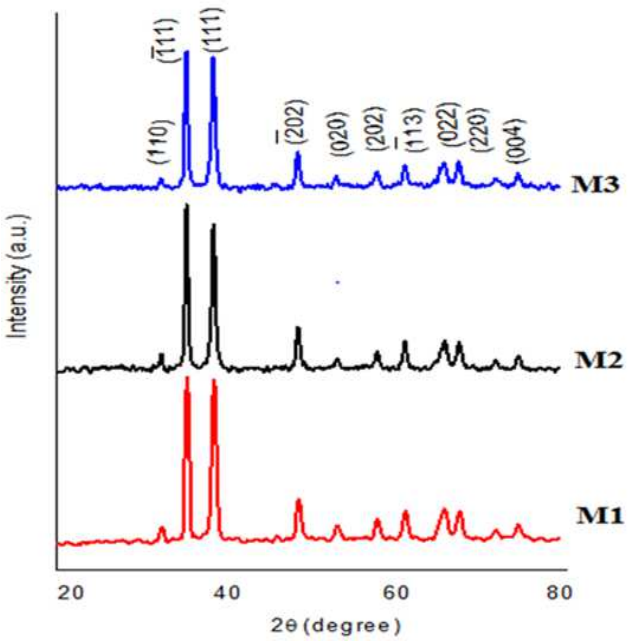


Fig. 1. Comparison of the powder XRD patterns of three different CuO NPs of M1, M2, and M3.

Figure 2 shows the comparison of UV-Visible absorption spectrums of the three different CuO NPs, where the characteristic surface plasmon resonance (SPR) peak can be observed at the wavelength of 343, 345, and 346 nm for the M1, M2, and M3 samples respectively. Also, by making use of the Tauc relationship, the optical direct bandgap of the produced NPs was calculated, i.e., a band energy gap of 3.28, 3.26, and 3.25 eV were observed for the M1, M2, and M3 samples respectively. The observation of such bandgap energy indicating the blue shift for all three samples' and the slight differences can be linked to the effects of crystal morphologies and associated quantum size effects [6].

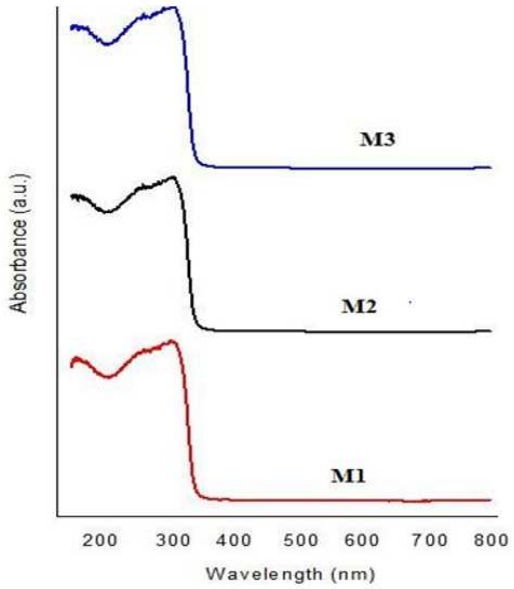


Fig. 2. UV-Vis absorption spectra of M1, M2, and M3 samples.

In the same way, Figure 3 compares the FTIR spectra of M1, M2, and M3 samples in the wavenumber range of 4000-500 cm-1. The observation of bands in the range of 3200-3800 $cm^{-1}$ in the spectrum may be attributed to the O-H stretching vibration caused by absorbed water/moisture. The $NH_3^+$ stretching vibration may be responsible for the bands observed around 2350-2360 $cm^{-1}$, while the C=O stretching vibration may be responsible for the bands observed around 1700-1710 $cm^{-1}$ [17]. In addition, the band observed around 1500 cm-1 may be due to the N-O asymmetric stretching vibration, while the characteristic band of Cu-O stretching toward the formation of CuO NPs is observed around 450 - 550 $cm^{-1}$ in all samples [18].

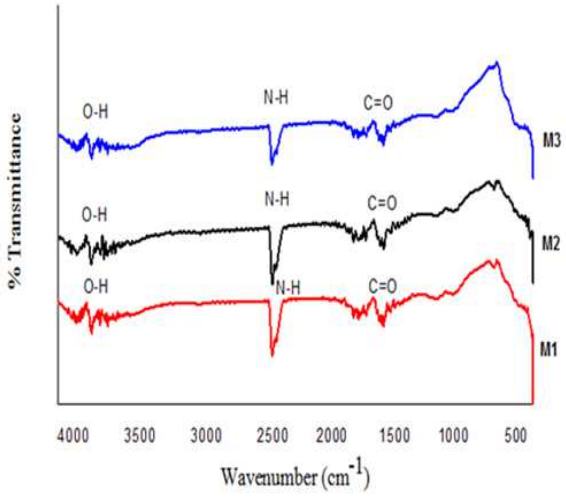


Fig. 3. Comparison of the FTIR spectra of M1, M2, and M3 samples.

Figure 4 shows the SEM images of three different CuO samples, where the images display for the bushes as flakes-like, wheat-like, and rice-like morphologies corresponding to M1, M2, and M3 samples, respectively. Also, from the observation of SEM provided morphologies, it can be indicated that the ratio of malic acid fuel plays a very important key role in tailoring the surface morphological properties, i.e., we observed different morphological patterns for all three samples and can be linked to the inherent effects of organic fuels. Since the aqueous combination of $Cu^{2+}$ ions and malic acid fuel in the initial stages leads to the formation of nucleation seeds first that further acts along with the growth of particles by serving as an initial nucleus. When the solution reached the maximum temperature (250°C), the malic acid's OH bonds serve as a template for the formation of CuO in a bush-like structure. The high temperature was gradually inherited after the malic acid ignited the combustion process and the particles of uniform size were obtained [19].

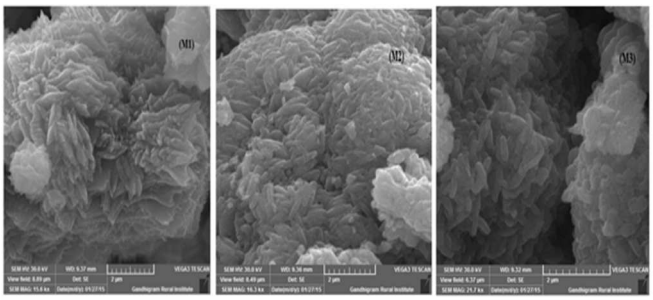

Fig. 4. SEM images of M1, M2, and M3 samples.

Further tests to investigate the antibacterial efficiency of the floral CuO NPs (CG) were carried against both gram-positive (B. cereus and S. aureus), gram-negative bacteria (E. coli and K. pneumoniae), and fungi (P. chrysogenum) as shown in Figure 5. When the inhibition zones formed by floral CuO NPs were compared to microbial strains, E. coli was found to have the greatest inhibitory effect, followed by K. pneumoniae, indicating that CuO has a stronger effect on gram-negative bacteria than gram-positive bacteria.

The electrostatic forces generated between the opposite charges, i.e., Cu ions with positive charges and negative charges of bacteria are responsible for the adhesion and bioactivity. On the treatment of CuO NPs to the strains in the liquid growth medium, the negatively charged peptidoglycans molecules get bound to the $Cu^{2+}$ ions; the E. coli bacteria being the gram-negative, allows for the reaching of a higher amount of $Cu^{2+}$ ions into reach the plasma membrane than that of the gram-positive bacteria [20]. Also, the bacterial cell membrane structure and the associated increase in the adhesion of bacteria, the gram-negative bacteria are less susceptible to the antibiotics and antibacterial agents than gram-positive bacteria [21]. In that way, the opposite electrical charges generated as a result of reduction at the bacterial cell wall are responsible for increased adhesion of CuO NPs and thereby exhibiting higher antibacterial activity. Further, the membrane thickness differences (peptidoglycan layer) among the gram-positive and gram-negative bacteria are responsible for the observed less effectiveness of Cu NPs against S. aura and B. cereus [22].

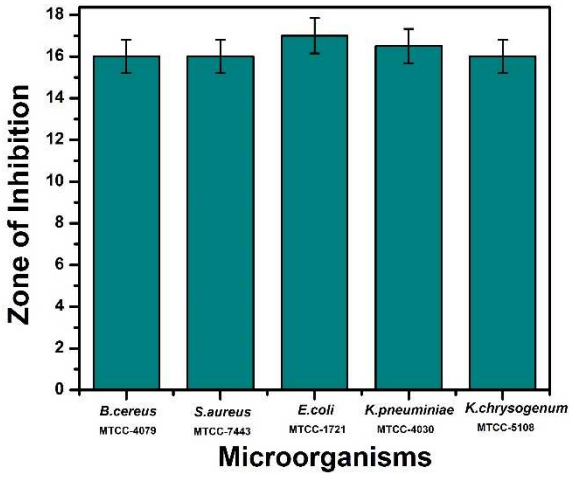


Fig. 5. Zone of inhibition (mm) of CuO NPs for various microorganisms.

## IV. CONCLUSION

In summary, the three different CuO NPs are being synthesized using the solution combustion method by applying changes in the fuel ratios (lower, stoichiometric, and higher). Powder XRD analysis reveals that all of the samples have a monoclinic crystal structure. The average grain size of CuO NPs are 17 nm for M1, 20 nm for M2, and 18 nm for M3. The UV-Vis analysis shows the maximum surface plasmon resonance peak for all the three samples were obtained with a bandgap of about 3.26 eV. According to the surface morphology analysis, the malic acid fuel ratio is vital in tailoring the surface morphology. Also, the floral CuO NPs' antibacterial activity was thoroughly explained by taking gram-positive, gram-negative, and fungi linked to the shape of NPs'.

## ACKNOWLEDGMENT

The authors extend their appreciation to University of Malaya for funding this work under grant number ST030-2019. The author Dr. A. Jegatha Christy is grateful to SERO/UGC for financial support.

## REFERENCES

[1] D Hariharan et al, J. Photochem. Photobiol. B Biol., 202(2020), 111636
[2] S. Sharon Tamil Selvi et al, J. Exp. Nanosci.,13(2018) 130- 143
[3] R. Sukhin Saravan et al, Optik, 207(2020) 164428
[4] R Thamiz Selvi et al, Mater. Res. Express 6 (2019) 125099
[5] D. Hariharan et al. J Mater Sci: Mater Electron 30, 12812-12819 (2019)
[6] M.Vidhya et al, Optik, 217(2020), 164878
[7] Abinaya Mathialagan et al, Optic. Mater., 100(2020)109643
[8] R Priya et al, Optik, 206 (2020) 164281
[9] M Muthukumaran et al, Mater. Res. Exp., 7 (2020) 015038
[10] M. Muthukumaran et al, Optik, 214 (2020) 164849
[11] Y Zou, Y Li, X Lian, and An Dongmin, Method Res. Mater. Sci. 3(2014) 44-51
[12] H-X Zhang, U. Siegert and R. Liu, W-B Cai, Nanoscale Res. Lett. 4 (2009) 705
[13] M Umadevi, and A Jegatha Christy, Spectrochimica Acta,109(2013) 133-137
[14] T Singanahally Aruna, and S Alexander Mukasyan, Solid State Mater. Sci. 12(2008) 44-50
[15] S Thakur, N Sharma, A Varkia, and J Kumar, Adv. App. Sci. Res. 5(4), (2014) 18-24
[16] P Mallick, and S Sahu, Nano. Sci. Nano. Tech. 2(2012) 71-84
[17] S Sankar, M R Manikandan, S D Gopal Ram, T Mahalingam, and G Ravi, J. Cryst. Growth, 312 (2010) 2729-2733
[18] Y Liu, Y Chu, M Li, L Lia, and L Dong, J. Mater. Chem, 16, (2006) 192-198
[19] A. Jegatha Christy, L.C. Nehru, M. Umadevi, Powder Technol., 235 (2013) 783-786
[20] K. Singh, Y. Kumar, P. Puri, M. Kumar, C .Sharma, Eur. J. Med. Chem. 52(2012) 313.
[21] H. Manikshete, S. K. Sarsamkar, S. A. Deodware, V. N. Kamble, M. R. Asabe, Inorg. Chem. Comm. 14 (2011) 618.
[22] G. Tong, M. Yulong, G. Peng, and X. Zirong, Vet. Microbiol. 105 (2005)113.